Arabian Journal of Chemistry (2017) **10**, 1061–1069

King Saud University

Arabian Journal of Chemistry

www.ksu.edu.sa
www.sciencedirect.com

ORIGINAL ARTICLE

Synthesis, characterization and metal coordination of a potential β-lactamase inhibitor: 5-Methyl-2-phenoxymethyl-3-*H*-imidazole-4-carboxylic acid (PIMA)

Chiara Romagnoli [a], Fabio Prati [a], Rois Benassi [b], Giulia Orteca [b], Monica Saladini [b], Erika Ferrari [b,*]

[a] *Department of Life Sciences and Geological Sciences, University of Modena and Reggio Emilia, via Campi, 103, 41125 Modena, Italy*
[b] *Department of Chemical and Geological Sciences, University of Modena and Reggio Emilia, via Campi, 103, 41125 Modena, Italy*

Received 26 August 2015; accepted 25 November 2015
Available online 2 December 2015

KEYWORDS

Imidazole based ligands;
Metal complexes;
β-Lactamase inhibitors;
UV–vis spectroscopy;
NMR spectroscopy;
DFT calculations

Abstract Among relevant metal ions in biological systems, zinc and iron play a key role as active partners of the catalytic machinery. In particular, the inhibition of metal enzymes that are involved in physiological and pathological processes has been deeply investigated for the rational design of selective and efficient drugs based on chelators. Since imidazole histidine residue is one of the most versatile sites in proteins, especially in enzymes acting in the presence of metal ions as cofactors, in this work the synthesis and characterization of a new imidazole derivative, namely 5-methyl-2-phenoxymethyl-3-*H*-imidazole-4-carboxylic acid (PIMA) is reported. PIMA was designed as metallo-β-lactamase inhibitor thanks to its similarity with penicillin V, a β-lactam antibiotic inactivated by metallo-β-lactamase, for which there are no commercially available inhibitors. The evaluation of PIMA coordinating ability toward iron, zinc, and gallium, these latter selected as a non-paramagnetic probe for iron, is performed by theoretical DFT calculations and in solution by experimental techniques, i.e. potentiometry, UV–vis and NMR spectroscopy. PIMA exhibits an efficient metal chelating ability; the prevailing species in physiological condition are ML_3 for Fe^{3+} and Ga^{3+} and ML_2 for Zn^{2+}, in which chelation is due to deprotonated carboxylic oxygen and imidazole nitrogen in the N,O donor set. The demonstrated ability of PIMA to chelate zinc ion,

* Corresponding author. Tel.: +39 0592058631.
E-mail address: erika.ferrari@unimore.it (E. Ferrari).
Peer review under responsibility of King Saud University.

Production and hosting by Elsevier

http://dx.doi.org/10.1016/j.arabjc.2015.11.007

combined with its structure similarity with penicillin V, supports further exploration of this imidazole-4-carboxylate as metallo-β-lactamase inhibitor.

1. Introduction

Imidazole histidine residue is one of the most versatile sites in proteins, especially in enzymes acting in the presence of metal ions as co-factors (Kapinos et al., 1998; Uchida, 2003; Remko et al., 2010; Li et al., 2010). The biological importance of imidazole moiety is therefore connected with its metal coordination ability; the metal complexes with several imidazole-containing ligands have also been studied as structural models for active sites of metallo-enzymes (Kimura et al., 1991; Jiang et al., 2006; Tagaki et al., 1993). Among relevant metal ions in biological systems, we can find zinc and iron, which represent the active partners of the catalytic machinery. These enzymes are involved in several physiological and pathological processes, and their inhibition, mainly based on metal chelation, has been deeply investigated for the rational design of selective and efficient drugs. For instance, within the family of zinc dependent enzymes, many efforts are reported for the inhibition of carbonic anhydrase, involved in edema and epilepsy (Alterio et al., 2012), matrix metallo-proteinases, for the treatment of pathologies such as arthritis and cancer (Dorman et al., 2010), or metallo-β-lactamases, to contrast the serious threat of antibiotic resistance (Phelan et al., 2014). Iron homeostasis involves a large number of proteins; thus, understanding their mechanisms of action allows the development of drugs useful for the treatment of pathologies related to iron dysregulation. Pharmacological strategies always include the formation of iron-chelate complexes that could compete with the biological storage sites of the metal itself. In addition, iron chelators may also be useful as anti-tumor agents, since they are able to deplete labile iron pool or cause oxidative stress in the tumor due to redox perturbations in its environment (Buss et al., 2003). Recently, studies have been conducted on neuroglobin, a new member of hemoprotein family, which takes part in many biological processes such as enzymatic reactions, signal transduction and the mitochondria function (Xu et al., 2009). As neuroglobin is associated with the mitochondria function, its potential therapeutic application in Alzheimer's disease and neurodegenerative disorders has been recently suggested (Liu et al., 2009). Differently from myoglobin and hemoglobin, neuroglobin has a hexacoordinated heme environment, with histidyl imidazole of proximal His^{96} and distal His^{64} directly bound to the metal ion.

The presence of substituents on the imidazole ring influences the basicity at the protonated nitrogen and this reflects on metal ligating ability. An interesting imidazole derivative is imidazole-4-acetic acid (IMA) which is a metabolite of histamine (Schayer, 1952) and histidine (Baldridge and Tourtellotte, 1958). This compound occurs in the brain of mammals and acts as a receptor activated by an inhibitor of neurotransmission-gamma-aminobutyric acid (GABA). It belongs to a newly separated class of receptors namely GABAc receptors whose action is modulated by transition metal ions (Ni^{2+}, Cu^{2+}, Cd^{2+}, Zn^{2+}) (Vien et al., 2002). From the bioinorganic point of view, IMA forms stable complexes with metal ions of biological relevance (Kurdziel et al., 2003; Sanna et al., 1998; Aljahdali et al., 2013). The presence of the azomethine nitrogen and carboxylic oxygen atoms in the molecule allows forming chelate complexes with metal ions although the crystal structure of Zn-IMA complex shows a polymeric arrangement (Drożdżewski et al., 2002).

This study reports the synthesis and characterization of a new imidazole derivative, namely 5-methyl-2-phenoxymethyl-3*H*-imidazole-4-carboxylic acid (PIMA), shown in Scheme 1.

This compound was designed as metallo-β-lactamase inhibitor thanks to its similarity with penicillin V, a β-lactam antibiotic inactivated by metallo-β-lactamase, for which there are no commercially available inhibitors (Cornaglia et al., 2011). In PIMA, the 2-phenoxymethyl-3-*H*-imidazole mimics the phenoxyacetylamino group in C6 of penicillin V, (Scheme 1) according to the well-known bioisosterism of this five-membered heterocycle with amides (Gordon et al., 1993). This similarity is also improved by the presence of the carboxylic group in position 4 of imidazole, recalling the hydrolysis product of penicillin V. Since in metallo-β-lactamase the catalytically active Zinc atom is coordinated by the penicillin

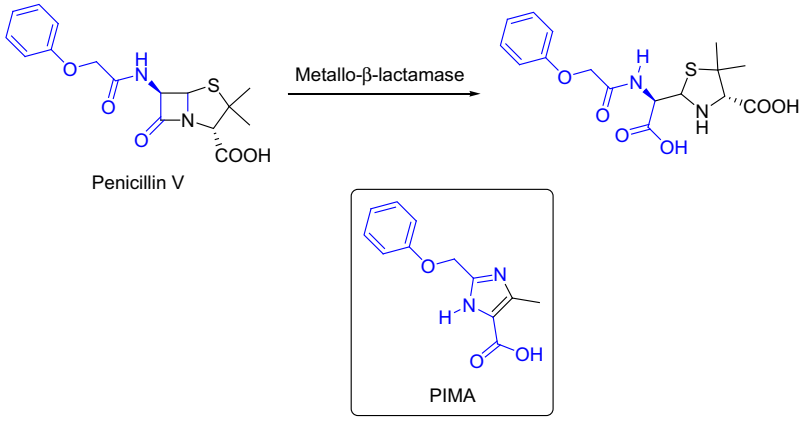

Scheme 1 Structural similarity of 5-methyl-2-phenoxymethyl-3-*H*-imidazole-4-carboxylic acid (PIMA) with Penicillin V.

β-lactam carbonyl (Page and Badarau, 2008), PIMA could represent a substrate analog inhibitor. In addition, this molecule represents a potential polydentate agent able to chelate metal ions in biological systems thanks to the presence in the molecular skeleton of donor atoms such as imidazole nitrogens, carboxylic oxygens and phenoxymethyl group. For all these reasons the evaluation of PIMA coordinating ability toward metal ions is of great relevance; hence, the solution study on Zn^{2+}, Fe^{3+} and Ga^{3+} containing systems is here reported together with DFT calculation.

2. Materials and methods

2.1. Synthesis

PIMA was obtained following Scheme 2.

The imidazole carboxylate (**1**), precursor of PIMA, can be easily obtained by one-pot reaction of a suitable 1,2-diaza-1,3-diene with 2-phenoxy-acetaldehyde and benzylamine as already described (Preti et al., 2010). The reaction implies the 1,5-electrocyclization of the in situ formed azavinyl azomethine ylide, promoted by microwave irradiation. The described intermediate **1** simply requires two deprotection steps to obtain the final compound: an initial hydrolysis furnishes the carboxy group, while the subsequent debenzylation unmasks the NH of imidazole.

Ethyl 3-benzyl-5-methyl-2-phenoxymethyl-3-*H*-imidazole-4-carboxylate (**1**) (840 mg, 2.40 mmol) was treated with a 2 M solution of sodium hydroxide in ethanol (3 mL, 6.00 mmol) and heated at reflux temperature for 2 h. The reaction mixture was then partitioned between water (20 mL) and diethyl ether (20 mL) and the aqueous phase was acidified with HCl 5% w/w. The precipitate formed was filtered and dried *in vacuo* overnight affording 3-Benzyl-5-methyl-2-phenoxymethyl-3*H*-imidazole-4-carboxylic acid (**2**) as a cream-colored solid (635 mg, 82%). M.p. 206–208 °C. ^{1}H NMR (400 MHz, CD_3-OD): δ 2.69 (3H, s, CH_3), 5.42 (2H, s, CH_2O), 5.92 (2H, s, NCH_2), 6.94 (2H, d, J 7.9, H_{Arom}), 7.05 (1H, t, J 7.6, H_{Arom}), 7.23 (2H, d, J 6.5, H_{Arom}), 7.29–7.40 (5H, m, H_{Arom}). ^{13}C NMR (100 MHz, CD_3OD): δ 10.5, 49.9, 59.6, 114.5 (2C), 121.6, 122.3, 126.5 (2C), 128.0, 128.7 (2C), 129.5 (2C), 134.3, 137.8, 144.6, 157.0, 159.5. MS (EI): m/z (%) 278 $[M–COOH]^+$ (1), 185 (46), 91 (100), 77 (3), 65 (17).

The previous intermediate **2** (604 mg, 1.87 mmol) was dissolved in methanol (120 mL) and palladium catalyst (Pd $(OH)_2$, 20 wt.% Pd on carbon, 604 mg) was added. The system was evacuated, purged with hydrogen and vigorously stirred for 16 h. The reaction mixture was then filtered and concentrated under reduced pressure, affording 5-methyl-2-phenoxymethyl-3-*H*-imidazole-4-carboxylic acid (PIMA) as a cream-colored solid (360 mg, 83%). M.p. 209–210 °C. ^{1}H NMR (400 MHz, DMSO-d_6): δ 2.42 (3H, s, CH_3), 5.07 (2H, s, CH_2O), 6.98 (1H, t, J 7.5, H_{Arom}), 7.05 (2H, d, J 7.5, HArom), 7.32 (2H, t, J 7.5, H_{Arom}). ^{13}C NMR (100 MHz, DMSO-d_6): δ 12.3, 62.4, 115.2 (2C), 121.7, 124.2, 130.0 (2C), 138.8, 143.4, 158.3, 163.2. MS (EI): m/z (%) 155 $[M–Ph]^+$ (1), 141 (3), 127 (5), 113 (4), 99 (17), 85 (50), 71 (69), 57 (100), 43 (61). Anal. Calculated for $C_{12}H_{12}N_2O_3$: C 62.00, H 5.21, N 12.12. Found%: C 61.72, H 5.18, N 12.87.

2.2. Potentiometric measurements

The aqueous solution of the PIMA (5.0×10^{-3} M) was obtained by water dilution of a methanolic solution (5.0×10^{-2} M); the concentration was determined potentiometrically. The percentage of methanol in the final solution was 10%. Potentiometric measurements were performed in aqueous solution at 25.0 ± 0.1 °C, using a fully automated ORION 960 Autochemistry System following the general procedures previously reported (Menabue et al., 1998). All experiments were carried out in a nitrogen atmosphere at an ionic strength of 0.1 M (adjusted with solid $NaNO_3$). Aqueous NaOH (0.01 M) or HNO_3 (0.01 M) was used as titrant. Ten titrations were performed with 40 data points in each titration in the range of pH 1–9. The protonation constants (β_{pq}) are defined in the following equations:

$$pL + qH \leftrightarrow L_pH_q \quad (1)$$

$$\beta_{pq} = [L_pH_q]/[L]^p[H]^q \quad (2)$$

where L is the ligand in the completely dissociated form and H is a proton Logβ_{pq} values were refined by least-squares calculation using the computer program HYPERQUAD (Gans et al., 1996).

2.3. Spectrophotometric measurements

UV–vis spectrophotometric measurements were performed using a Jasco V-570 spectrophotometer at 25 ± 0.1 °C in the 200–400 nm spectral range employing 1 cm quartz cells.

Spectrophotometric titrations were performed using 5.0×10^{-4} M solution of PIMA obtained by water dilution of a freshly prepared methanolic solution (5.0×10^{-2} M) with addition of an appropriate amount of a aqueous solution of the metal ion (5×10^{-2} M; 1:1, 1:2 and 1:3 M:L molar ratios). The amount of methanol in the final solution was 1%; hence, it was used as an aqueous solution. The pH-metric titrations of the ligand and metal–ligand systems were obtained varying the pH value by adding small amounts of concentrated NaOH

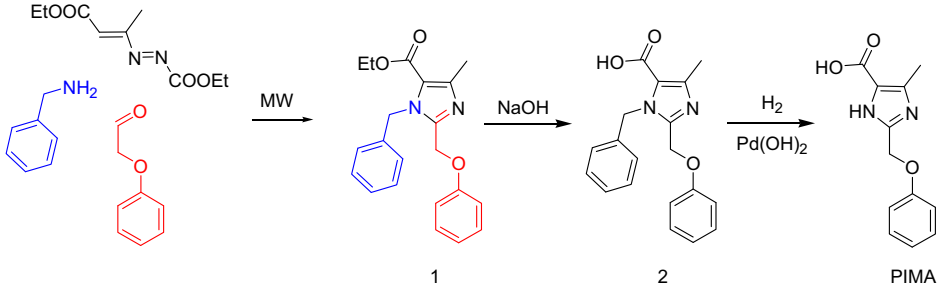

Scheme 2 Synthesis of PIMA.

or HCl in the pH range 2–9 (total number of different pH values ranging from 20 to 25 in each titration). A constant ionic strength of 0.1 M ($NaNO_3$) was maintained in all experiments. Each titration was repeated three times. The overall stability constants (expressed as $\log\beta_{MLH}$) were refined from spectrophotometric data by least-squares calculation using the software HypSpec (Gans et al., 1999), and taking into account the presence of the species $[Fe(OH)]^{2+}$; $[Fe(OH)_2]^{+}$; $[Fe_2(OH)_2]^{4+}$ (Escandar et al., 1994).

2.4. NMR spectroscopy

NMR spectra were recorded on a Bruker Avance AMX-400 spectrometer with a Broad Band 5 mm probe in inverse detection. Nominal frequencies were 100.13 MHz for ^{13}C, and 400.13 MHz for ^{1}H. For each sample, 0.5 mL of mM solution was prepared in MeOD-d_4. The synthesis of Ga^{3+}:PIMA complex in MeOD-d_4 was obtained *in situ*, by adding to mM ligand solution (0.5 mL) the proper addition of $Ga(NO_3)_3$ solution to reach the 1:1 metal to ligand molar ratio. Spectra were registered after few minutes from the addition. Typical parameters were used for 2D COSY, HSQC, and HMBC experiments.

2.5. Computational details

All calculations were performed with the Gaussian 03 package of programs (Frisch et al., 2004) and GaussView 03 (Dennington et al., 2003) used as the plotting tool for data visualization. The computations were performed by DFT approaches, and the structures were fully optimized using hybrid-functional B3LYP applied to the 6-311G** basis set (B3LYP/6-311G**).

3. Results and discussion

3.1. Acid–base equilibria

The acid–base equilibria of PIMA are reported in Scheme 3.

The analysis of potentiometric data yields two pK_a values corresponding to the dissociation of carboxylic and protonated imidazole groups [pK_{a1} = 2.78(2), pK_{a2} = 5.81(2)] (Fig. 1S).

The spectrophotometric titration of PIMA (Fig. 1) shows a significant increase in absorbance at λ 260 nm and λ 300 nm with increasing pH; by plotting A *vs.* pH a titration trend is observed although the unique clearly visible equivalent point is the dissociation of the protonated imidazole group. By processing the data with HySpec program (Gans et al., 1999) two pK_a are obtained [pK_{a1} = 2.91(2) pK_{a2} = 5.84(2)] whose values are in good agreement with the potentiometrically found data. pK_{a1} value is near to that found for IMA (Sanna et al., 1998; Várnagy et al., 1994) while pK_{a2} is lower than the value found for IMA (7.34(1), 7.12(4) (Aljahdali et al., 2013) and is lower also with respect to free imidazole (6.95) (Várnagy et al., 1994) or imidazole-4-carboxylic acid (6.28) (Podsiadly, 2008). The greater value of IMA with respect to imidazole was previously attributed to the formation of an intramolecular hydrogen bond involving the protonated imidazole N and the carboxylate group (Aljahdali et al.), even though in the crystal structure of hydrated IMA reported by Okabe and Hayashi (1999) there is no evidence of intramolecular hydrogen bond. Hence, the structure of IMA in solution still remains unclear. In our case, the presence of an electron-withdrawing group such as the phenoxymethyl contributes to increase the acidity of NH^{+} hydrogen.

3.2. Metal complexation

The metal complexation was studied by means of ^{1}H NMR and spectrophotometric titrations while potentiometric analy-

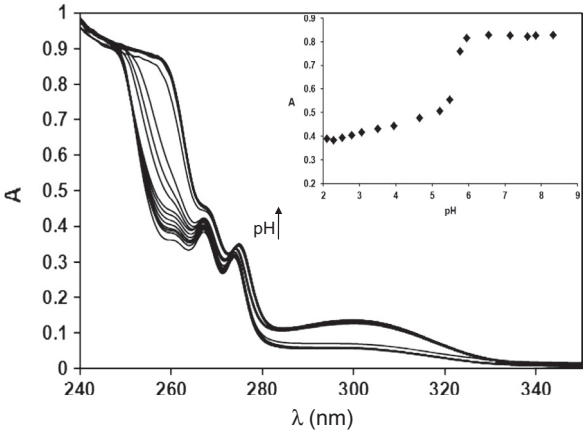

Figure 1 Spectrophotometric titration of an aqueous solution of PIMA 5×10^{-4} M, the inset shows the plot of absorbance (A) *vs.* pH at λ = 260 nm.

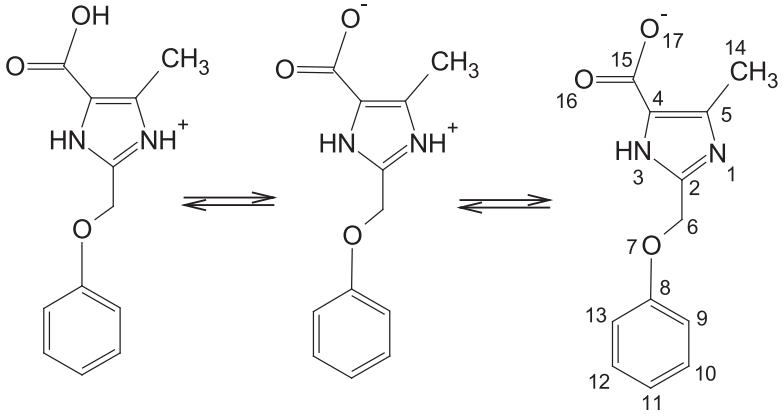

Scheme 3 Neutral and ionic form of PIMA with atom numbering scheme.

sis was prevented by the poor water solubility of the metal complex species in the investigated pH range.

PIMA shows the typical ^{1}H NMR spectral pattern of substituted imidazoles (see experimental section). $Ga(NO_3)_3$ is used as NMR probe for Fe^{3+} (Atkinson et al., 1998; Hara et al., 2000), and its addition to a solution of PIMA at acidic pH, immediately originates a complex species, whose spectral pattern resembles one of the free ligands, but it is downfield shifted (Fig. 2). The greater downfield shift is observed for methylenic (H-6) and methylic (H-14) protons, and this behavior should be principally due to the formation of a metal complex, which is in fast exchange with the free ligand in the NMR timescale.

By reaching the Ga^{3+}:PIMA 1:3 M ratio no further downfield shift is observed but a new set of signals appears, attributed to a complex species at M:L 1:2 M ratio while the M:L 1:3 metal complex, observed at downfield, represents a minor species.

As far as Gallium ion is added a new set of signals which are attributed to the formation of M:L 1:1 species appears at higher field than M:L 1:2 complex species. From this point onward, the metal-complex species present in solution exchange fast between each other with respect to the NMR timescale, then the addition of Ga^{3+} varies speciation distribution as observed by the change in signals' integrated areas. Upon reaching M:L 1:1 the three complex species at M:L 1:1, 1:2 and 1:3 are simultaneously present with the prevalence of 1:1 and 1:3 M ratio.

The ^{1}H ^{13}C hetero correlated spectra reported in Fig. 3 (Panel A and B) show that the most significant shifts are observed for H-6 protons while the phenyl protons and C8 are only poorly affected. This finding suggests the involvement of both carboxylic group and imidazole nitrogen in metal coordination with the formation of a five-membered metallacycle.

Spectrophotometric titration was performed by adding Ga^{3+}, Fe^{3+} and Zn^{2+} to a methanolic-aqueous solution (1:100 V/V) of the ligand. Fig. 4 reports the spectra of Fe^{3+}:PIMA system; at each addition of metal ion there is an increase in absorbance which reaches the maximum value at the M:L 1:1 M ratio (inset Fig. 4).

Increasing pH in the M:PIMA 1:2 M ratio system for all metal ions (Fig. 5 reports the titration for Fe^{3+}:PIMA system), an increase in absorbance at λ 300 nm is observed confirming that the formation of metal complex is pH dependent. At pH 4 the complex species is completely formed as the absorbance reaches its maximum value. This absorption band was attributed to the dissociation of protonated imidazole group; therefore, we can confirm that metal complexation involves imidazole nitrogen and the replacement of hydrogen by the metal ion occurs at a pH value significantly lower compared to the dissociation of the free ligand (pH $\sim$ 4 *vs.* pH $\sim$ 5.8). Over pH 8 the competition with hydroxyl anion becomes significant and, in this working concentration, the formation of metal hydroxide takes place.

From the spectrophotometric titration of M^{n+}:PIMA system in 1:1, 1:2 M ratio for $n = 2$ and 1:3 M ratio for $n = 3$ the stability constants of the complex species are evaluated taking into account different types of protonated and neutral species; best convergence of data was reached considering the $\log\beta$ values reported in Table 1.

Fig. 6 reports the species distribution curves for Fe^{3+}, Ga^{3+} and Zn^{2+} containing systems. The prevailing species in physiological condition is ML_3 for Fe^{3+} and Ga^{3+} and

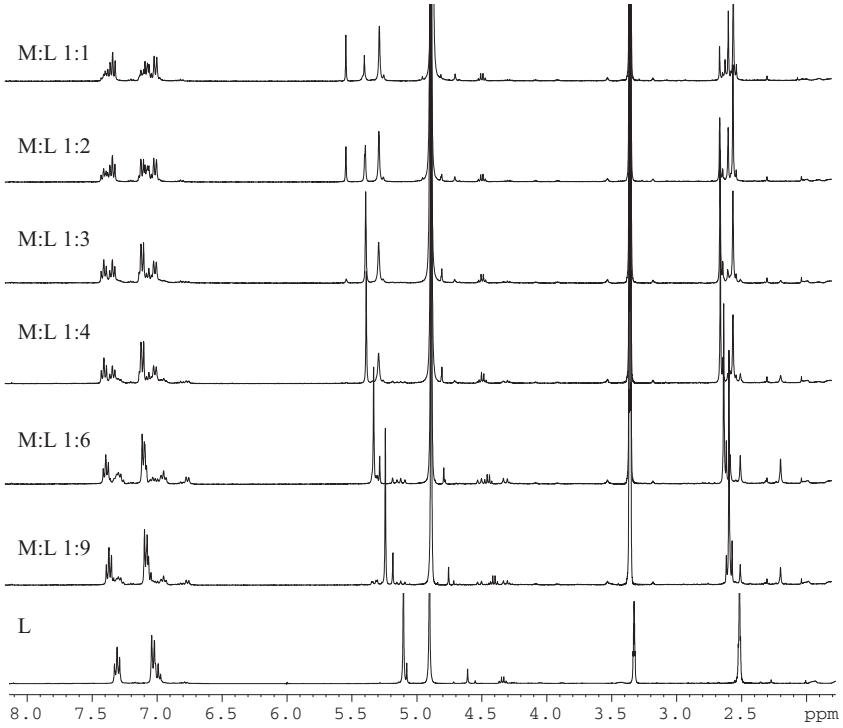

Figure 2 ^{1}H NMR titration of PIMA with Ga^{3+} in MeOD-d_4. From bottom (free ligand), spectra obtained by progressive additions of metal ion to the ligand up to metal to ligand 1:1 M ratio (top spectrum).

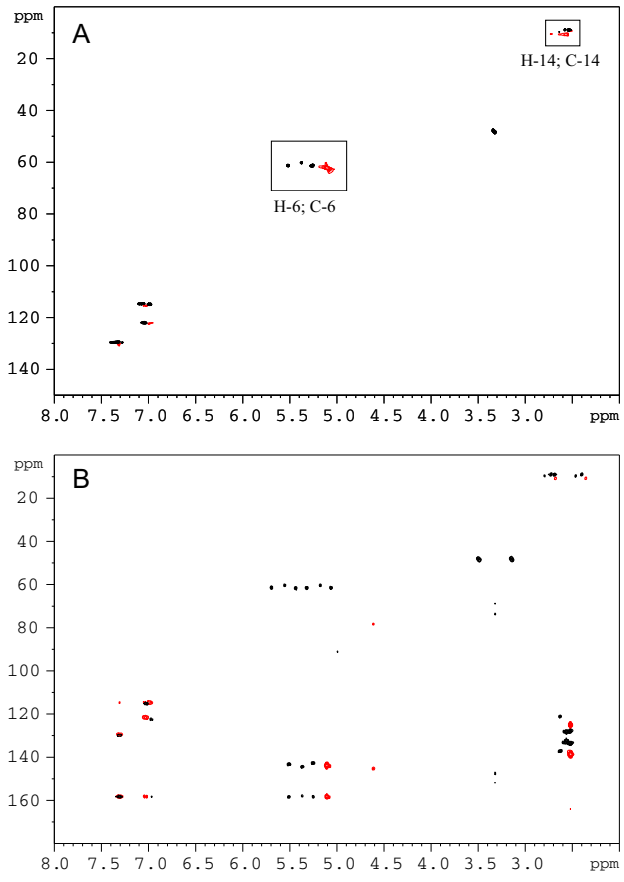

Figure 3 Panel A: Overlap of $^{1}H–^{13}C$ HSQC (Hetero-nuclear Single Quantum Coherence) spectra of free PIMA (red) and Ga^{3+}:PIMA 1:1 system (black). Panel B: Overlap of $^{1}H–^{13}C$ HMBC (Hetero-nuclear Multiple Bond Coherence) spectra of free PIMA (red) and Ga^{3+}:PIMA 1:1 system (black). All spectra were acquired in MeOD-d_4 at 298 K.

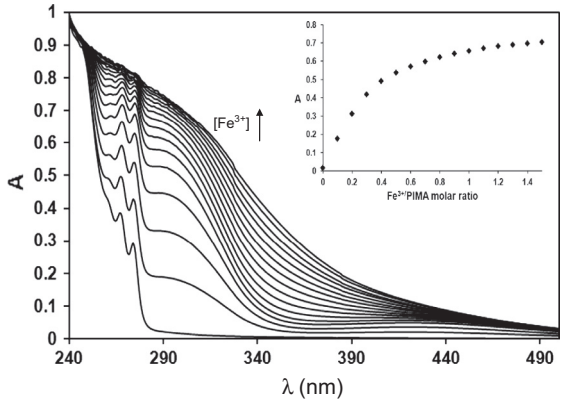

Figure 4 Spectrophotometric titration of PIMA 5×10^{-4} M with Fe^{3+}, [Fe^{3+}] increasing from bottom to top. Inset shows the plot of absorbance (A) *vs.* M/L molar ratio at λ 300 nm.

ZnL_2, in which PIMA coordinates the metal ion through deprotonated carboxylic oxygen and imidazole nitrogen, as it was proposed by NMR data.

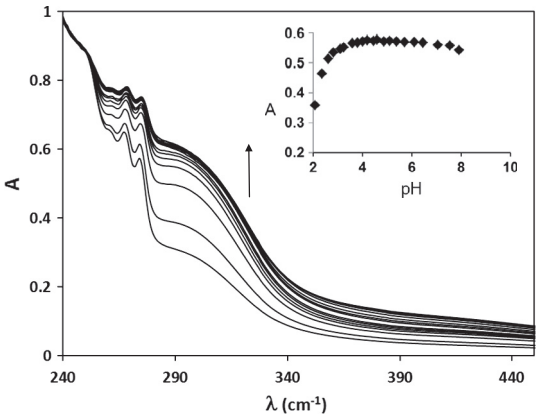

Figure 5 pH-metric spectrophotometric titration of Fe^{3+}:PIMA system in 1:2 M ratio, inset shows the plot of absorbance *vs.* pH at λ 300 nm; [Fe^{3+}] 2.5×10^{-4} M.

The formation of a chelate complex is consistent with the high $\log K^{Zn}_{ZnL}$ QUOTE value compared to QUOTE $\log K^{H}_{HL}$ of PIMA as suggested by Sigel et al. (2000). This coordination behavior was found also for imidazole-4-carboxylic acid toward V^{3+} ion in solution (Podsiadly, 2008). In the solid state IMA forms chelate complexes with Co^{2+} and Mn^{2+} ions (Kurdziel et al., 2003) while with Zn^{2+}, in acidic conditions, it was found to give polymeric arrangement in which one anionic ligand molecule bridges two Zn(II) ions and the second neutral ligand acts as monodentate through carboxylic oxygen (Drożdżewski et al., 2002). The stability constants of Zn(II) complexes are comparable to those found for the corresponding species with IMA by Török et al. (1998) ($\log \beta_{110}$ 3.81 and $\log \beta_{120}$ 7.15), in which the suggested N,O coordinating mode was attributed to imidazole nitrogen and carboxylic oxygen. A comparison with similar, but not imidazole-based ligands, such as β-ala, evidences how the imidazole ring greatly increases the stability of metal complexes.

The stability constants of Fe^{3+} PIMA complexes are similar to those observed by Farkas et al. (2007) for the corresponding complexes with imidazole-4-carbohydroxamic acid ($\log \beta_{110}$ 10.46(1) and log $\log \beta_{111}$ 12.1(1)) in which the chelate coordination mode involves only $O_{hydroxamate}$ atoms. In the investigated system, imidazole-4-carbohydroxamic acid resulted competitive with hydroxide ion in binding Fe(III), and precipitation phenomena were attributed to the formation of low water-soluble polynuclear complexes rather than iron-hydroxo species. The $\log \beta_{110}$ for PIMA is greater than the corresponding one for carboxylate complexes, and this suggests a possible involvement of imidazole nitrogen in stabilizing the metal complex, and particularly a remarkable π-acceptor property of imidazole ring, as suggested by Török et al. (1998). The precipitation of hydroxo species was only observed above pH 9, suggesting the immobilization of iron by PIMA in the experimental conditions applied for spectrophotometric titrations. Differently from the cited system, in our case also a FeL_3 complex is found, which prevails at physiological pH as well as for Ga^{3+}, consistently with NMR data. Ga^{3+} ion gives less stable species than Fe^{3+}; this trend was previously found for other chelated complexes with O-donor ligands (Ferrari et al., 2013). According to species distribution curves, PIMA seems a good iron chelator at physiological pH, at least in the exper-

Table 1 Logarithms of protonation constants of PIMA and logarithms of formation constants of metal complexes at 25 °C, $I = 0.1$ M ($NaNO_3$).

	$\log\beta_{MHL}$		Fe^{3+}	Ga^{3+}		Zn^{2+}
HL	$\log\beta_{011}$	5.84(2)				
H_2L^+	$\log\beta_{012}$	8.75(2)				
ML^{2+}	$\log\beta_{110}$		11.34(2)	10.71(4)	ZnL^+	5.01(1)
MHL^{3+}	$\log\beta_{111}$		14.23(2)	14.01(2)	$ZnHL^{2+}$	7.80(2)
ML_2^+	$\log\beta_{120}$		20.21(3)	19.87(2)	ZnL_2	9.81(2)
$M(HL)_2^{3+}$	$\log\beta_{122}$		28.01(2)	27.84(3)	$Zn(HL)_2^{2+}$	14.3(1)
ML_3	$\log\beta_{130}$		24.72(3)	23.89(3)		
$M(HL)_3^{3+}$	$\log\beta_{133}$		41.20(2)	40.12(2)		

imental conditions applied for spectrophotometric measurements. A more proper indicator of the Fe^{3+} sequestering ability in physiological conditions is represented by pFe^{3+} defined as $-\log[Fe^{3+}]$ (Liu and Hider, 2002).

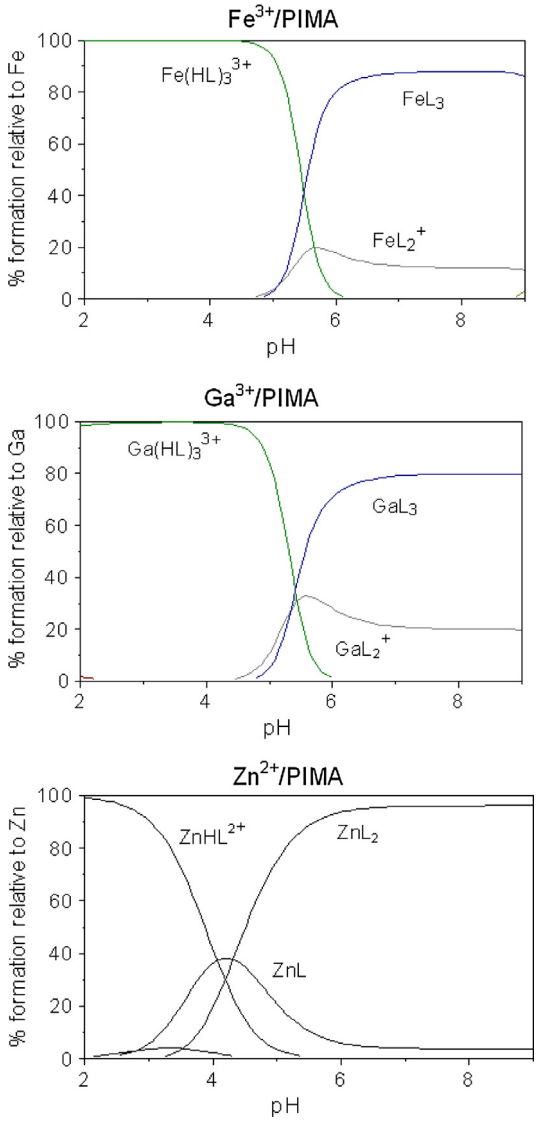

Figure 6 Species distribution curves for M:L systems $[M]_{tot} = 2.5 \times 10^{-4}$; $[L]_{tot} = 5 \times 10^{-4}$.

Table 2 reports the pFe^{3+} values for several hexadentate and bidentate ligands, which are effective iron chelators for therapeutic applications (Liu and Hider, 2002). Hexadentate ligands show greater pFe^{3+} values but they have the disadvantage of a high molecular weight.

Among bidentate ligands hydroxypyridinones present a great effectiveness in iron chelation conjugated with a low molecular mass. The key property for orally active iron chelator is its ability to be efficiently absorbed from the gastrointestinal tract (GIT) and to cross biological membranes. The molecular size is a critical factor, which influences the rate of drug absorption: with respect to the molecular weight "cut-off" (ca. 500 Da) for the paracellular route absorption in the human small intestine (Liu and Hider, 2002) PIMA (232 Da) could reach the target sites at sufficient concentration.

3.3. DFT calculations

Fig. 7 shows the optimized structures for different conformers of PIMA and Table 3 reports the total energy values (E) and relative energy values (ΔE) of the different conformers and relative monoanion. The most stable conformer **A** is probably stabilized by an attractive interaction involving H(N3) and carboxylic oxygen, in addition to the planarity of the molecule, shown by the dihedral angle N3–C2–C6–O7 (Table 2, atom numbering as in Scheme 2). A similar interaction was found in a theoretical study on different imidazole carboxylic acids (Alkorta and Elguero, 2005).

Previous crystal data of imidazole-4-acetic acid monohydrate showed IMA in the zwitterionic form in the solid state

Table 2 Comparison of pFe^{3+} values and stability constants for bidentate (b) and hexadentate (h) ligands. Values taken from Liu and Hider (2002).

Ligand	Denticity	$\log\beta_{13}$	pFe^{3+}
PIMA	b	24.72	17
DMB (N,N-dimethyl-2,3-dihydroxybenzamide)	b	40	15
1-Methyl-3-hydroxy-4-pyridinone	b	32	16
1,2-Dimethyl-3-hydroxy-4-pyridinone	b	37.2	19
MECAM (mesitylene catecholamine)[a]	h	43	28
DFO (desferrioxamine)[a]	h	31	26

$pFe^{3+} = -\log [Fe^{3+}]$; $[Fe^{3+}]_{total} = 10^{-6}$ M; $[L]_{total} = 10^{-5}$ M; pH 7.4.

[a] $\log\beta$ is referred to 1:1 complex.

(Okabe and Hayashi, 1999) stabilized by hydrogen bonds involving water molecules. In the anionic form of both *A* and *B* conformers the planarity of the molecule is removed being the dihedral angle of 68.80° and 52.72° respectively, even if the hydrogen bond interaction between H(N3) and carboxylic oxygen is retained.

In order to calculate the most plausible structure of PIMA metal complexes, we have taken into account the $B(H_{-1})$ anion, which is the only one able to interact with metal ion leading to the formation of a chelate complex. Actually, the involvement of N3 in metal coordination requires the proton dissociation that cannot be proposed under the pH conditions in which the present study was carried out.

Considering the stoichiometry of the prevailing species at physiological pH and assuming the coordination mode suggested by NMR data we also calculated the structure for Ga $(PIMA)_3$ shown in Fig. 8, together with the total energy value (*E*) and the binding energy value (BE) of the complex. Apparently, no examples of DFT calculations on Ga(III) complexes with N,O donor atoms are reported in the literature; however, the BE value of $Ga(PIMA)_3$ is of the same order of magnitude with respect to that found for Ga(III) complexes with curcumin 1347.73 kcal/mol and curcumin derivatives 1354.22 kcal/mol (Ferrari et al., 2014).

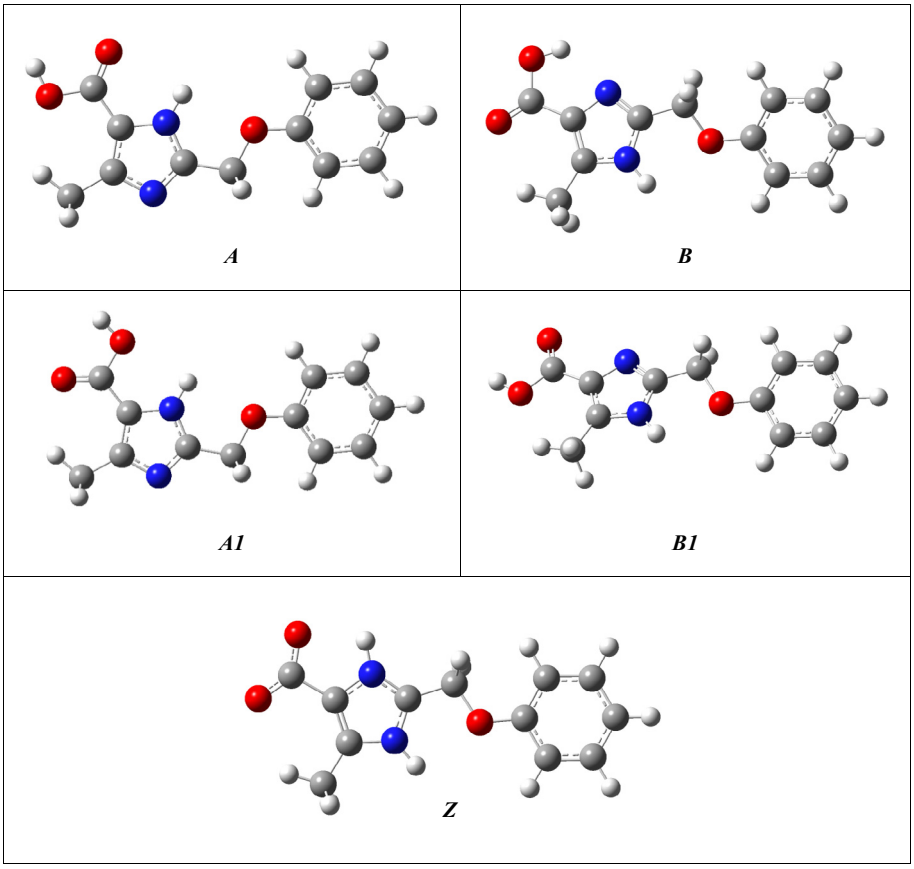

Figure 7 Optimized structures at B3LYP/6-31G** level of different tautomers of PIMA and its monoanion (*Z*).

Table 3 B3LYP/6-311G** total energy *E* (a.u.) and relative energy Δ*E* (kcal/mol) for different conformers of neutral PIMA and its monoanion. *A*, *B*, and *Z* conformers are referred to Fig. 7; dihedral angle N3–C2–C6–O7.

Neutral PIMA				PIMA anion			
	E (a.u.)	Δ*E* (kcal/mol)	Dihedral angle (°)		*E* (a.u.)	Δ*E* (kcal/mol)	Dihedral angle (°)
A	−799.719735	0	0	$A(H_{-1})$	−799.157108	0	68.80
*A*1	−799.719400	0.21	23.56	$B(H_{-1})$	−799.132914	15.18	52.72
B	−799.718915	0.52	24.03				
*B*1	−799.712751	4.38	23.56				
Z	−799.674572	28.34	−0.13				
*Z*1	−799.678193	26.07	7.63				

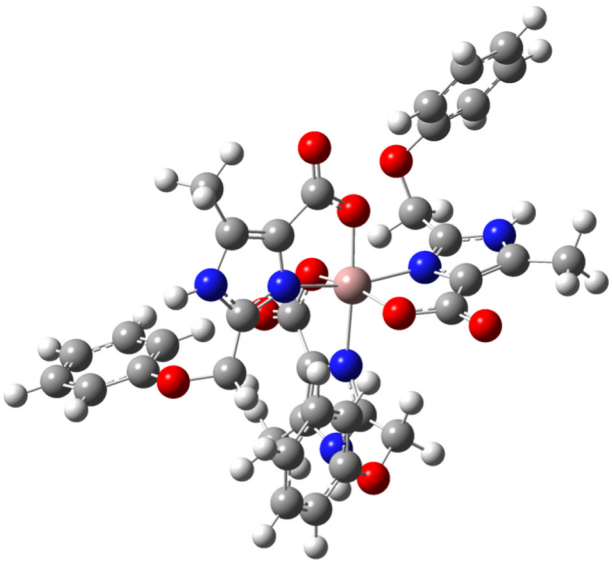

Figure 8 Optimized structures at B3LYP/6-31G** level of Ga $(PIMA)_3$ complex. TEc – 4320.481825 (a.u.); BE 1452.61 (kcal/mol). Where BE = TE_S – TE_C where TE_S = sum of the total electronic energy of the bare metal ion and the relative isomer of the complexing anion (a.u.); TE_C = total electronic energy of complexes (a.u.).

4. Conclusions

UV–vis and NMR spectroscopic data highlighted that PIMA exhibits an efficient metal chelating ability toward different metal ions of great biological relevance such as iron and zinc. The good stability of the formed complexes at physiological pH suggests the possible use of PIMA for therapeutic applications as chelator, especially for iron. In particular, the demonstrated ability of PIMA to chelate zinc ion, combined with its structure similarity with penicillin V, supports further exploration of this imidazole-4-carboxylate as metallo-β-lactamase inhibitor.

Acknowledgments

The authors are grateful to the "Centro Interdipartimentale Grandi Strumenti – C.I.G.S." of the University of Modena and Reggio Emilia and to the "Fondazione Cassa di Risparmio di Modena" for supplying NMR and mass spectrometers.

Appendix A. Supplementary material

Supplementary data associated with this article can be found, in the online version, at http://dx.doi.org/10.1016/j.arabjc.2015.11.007.

References

Aljahdali, M., El-Sherif, A.A., Shoukry, M.M., Mohamed, S.E., 2013. J. Sol. Chem. 42, 1028.
Alkorta, I., Elguero, J., 2005. Struct. Chem. 16, 507.
Alterio, V., Di Fiore, A., D'Ambrosio, K., Supuran, C.T., De Simone, G., 2012. Chem. Rev., 4421
Atkinson, R.A., El Din, A., Kieffer, B., Lefevre, J.F., Abdallah, M.A., 1998. Biochemistry 37, 15965.
Baldridge, R.C., Tourtellotte, C.D., 1958. J. Biol. Chem. 233, 125.
Buss, J.L., Torti, F.M., Torti, S.V., 2003. Curr. Med. Chem. 10, 1021.
Cornaglia, G., Giamarellou, H., Rossolini, G.M., 2011. Lancet Infect. Dis. 11, 381–393.
Dennington II, R., Keyth, T., Millam, J., Eppinnett, K., Hovell, W.L., Gilliand, R., 2003. Gaussview, Version 3.0, Semichem Inc, Shawnee Mission, KS.
Dorman, G., Cseh, S., Hajdu, I., Barna, L., Konya, D., Kupai, K., Kovacs, L., Ferdinandy, P., 2010. Drugs 70, 949.
Drożdżewski, P., Pawalk, B., Głowiak, T., 2002. Polyhedron 21, 2819.
Escandar, G.M., Olivieri, A.C., Gonzales-Sierra, M., Sala, L.F., 1994. J. Chem. Soc., Dalton Trans., 1189
Farkas, E., Bátka, D., Csóka, H., Nagy, N.V., 2007. Bioinorg. Chem. Appl., http://dxdoi.org/10.1155/2007/96536.
Ferrari, E., Asti, M., Benassi, R., Pignedoli, F., Saladini, M., 2013. Dalton Trans. 42, 5304.
Ferrari, E., Benassi, R., Sacchi, S., Pignedoli, F., Asti, M., Saladini, M., 2014. J. Inorg. Biochem. 139, 38.
Frisch, M.J., Trucks, G.W., Schlegel, H.B., Scuseria, G.E., et al., 2004. Gaussian 03, Revision D.01, Gaussian Inc, Wallingford CT.
Gans, P., Sabatini, A., Vacca, A., 1996. Talanta 43, 1739.
Gans, P., Sabatini, A., Vacca, A., 1999. Ann. Chim. 89, 45.
Gordon, T., Hansen, P., Morgan, B., Singh, J., Baizman, E., Ward, S., 1993. Bioorg. Med. Chem. Lett. 3, 915.
Hara, Y., Shen, L., Tsubouchi, A., Akiyama, M., Umemoto, K., 2000. Inorg. Chem. 39, 5074.
Jiang, H.Y., Zhou, C.H., Luo, K., Chen, H., Lan, J.B., Xie, R.G., 2006. J. Mol. Catal. A 260, 288.
Kapinos, L.E., Song, B., Sigel, H., 1998. Inorg. Chim. Acta 280, 50.
Kimura, E., Kurogi, Y., Shionoya, M., Shira, M., 1991. Inorg. Chem. 30, 4524.
Kurdziel, K., Głowiak, T., Materazzi, S., Jezierska, J., 2003. Polyhedron 22, 3123.
Li, F., Fitz, D., Fraser, D.G., Rode, B.M., 2010. Amino Acids 38, 287.
Liu, J., Yu, Z., Guo, S., Lee, S.R., Xing, C., Zhang, C., Gao, Y., Nicholls, D.G., Lo, E.H., Wang, X., 2009. J. Neurosci. Res. 87, 164.
Liu, Z.D., Hider, R.C., 2002. Coord. Chem. Rev. 232, 151.
Menabue, L., Saladini, M., Ugoletti, N., 1998. J. Inorg. Biochem. 69, 217.
Okabe, N., Hayashi, T., 1999. Acta crystallogr. Sect. C 55, 1142.
Page, M., Badarau, A., 2008. Bioinorg. Chem. Appl., http://dxdoi.org/10.1155/2008/576297.
Phelan, E.K., Miraula, M., Selleck, C., Ollis, D.L., Schenk, G., Mitić, N., 2014. Am. J. Mol. Biol. 4, 89.
Podsiadly, H., 2008. Polyhedron 27, 1563.
Preti, L., Attanasi, O.A., Caselli, M., Favi, G., Ori, C., Davoli Felluga, F., Prati, F., 2010. Eur. J. Org. Chem. 22, 4312.
Remko, M., Fitz, D., Rode, B.M., 2010. Amino Acids 39, 1309.
Sanna, D., Micera, G., Buglyò, P., Kiss, T., Gajda, T., Surdy, P., 1998. Inorg. Chim. Acta 268, 297.
Schayer, R.W., 1952. J. Biol. Chem. 196, 469.
Sigel, H., Saha, A., Saha, N., Carloni, P., Kapinos, L.E., Griesser, R., 2000. J. Inorg. Biochem. 78, 129.
Tagaki, W., Ogino, K., Fujita, T., Yoshida, T., Nishi, K., Inaba, Y., 1993. Bull. Chem. Soc. Jpn. 66, 140.
Török, I., Sturdy, P., Rockenbauer, A., Korecz Jr, L., Anthony, G.J., Koolhaas, A., Gajda, T., 1998. J. Inorg. Biochem. 71, 7.
Uchida, K., 2003. Amino Acids 25, 249.
Várnagy, K., Sóvágó, I., Ágoston, K., Likó, Z., Süli-Vargha, H., Sanna, D., Micera, G., 1994. J. Chem. Soc. Dalton Trans., 2939
Vien, J., Duke, R.K., Mewett, K.N., Johnston, J.A.R., Shingai, R., Chebib, M., 2002. Br. J. Pharmacol. 135, 883.
Xu, J., Li, L., Yin, G., Li, H., Du, W., 2009. J. Inorg. Biochem. 103, 1693.